# Influence of Cu Content on Compound Formation near the Chip Side for the Flip-Chip Sn-3.0Ag-(0.5 or 1.5)Cu Solder Bump during Aging

GUH-YAW JANG,[1] JENQ-GONG DUH,[1,5] HIDEYUKI TAKAHASHI,[2] SZU-WEI LU,[3] and JEN-CHUAN CHEN[4]

1.—Department of Materials Science and Engineering, National Tsing Hua University, Hsinchu, Taiwan. 2.—Application & Research Center, JEOL Ltd., Tokyo, Japan. 3.—Flip-Chip Engineering Department, TSMC Ltd., Hsinchu, Taiwan. 4.—Flip-Chip Operation, ASE, Chung-Li, Taiwan. 5.—E-mail: jgd@mx.nthu.edu.tw

Sn-Ag-Cu solder is a promising candidate to replace conventional Sn-Pb solder. Interfacial reactions for the flip-chip Sn-3.0Ag-(0.5 or 1.5)Cu solder joints were investigated after aging at 150°C. The under bump metallization (UBM) for the Sn-3.0Ag-(0.5 or 1.5)Cu solders on the chip side was an Al/Ni(V)/Cu thin film, while the bond pad for the Sn-3.0Ag-0.5Cu solder on the plastic substrate side was Cu/electroless Ni/immersion Au. In the Sn-3.0Ag-0.5Cu joint, the Cu layer at the chip side dissolved completely into the solder, and the Ni(V) layer dissolved and reacted with the solder to form a $(Cu_{1-y},Ni_y)_6Sn_5$ intermetallic compound (IMC). For the Sn-3.0Ag-1.5Cu joint, only a portion of the Cu layer dissolved, and the remaining Cu layer reacted with solder to form $Cu_6Sn_5$ IMC. The Ni in Ni(V) layer was incorporated into the $Cu_6Sn_5$ IMC through slow solid-state diffusion, with most of the Ni(V) layer preserved. At the plastic substrate side, three interfacial products, $(Cu_{1-y},Ni_y)_6Sn_5$, $(Ni_{1-x},Cu_x)_3Sn_4$, and a P-rich layer, were observed between the solder and the EN layer in both Sn-Ag-Cu joints. The interfacial reaction near the chip side could be related to the Cu concentration in the solder joint. In addition, evolution of the diffusion path near the chip side in Sn-Ag-Cu joints during aging is also discussed herein.

**Key words:** Flip chip, interfacial reaction, Sn-Ag-Cu solder

## INTRODUCTION

With concerns about the toxic effects of Pb on human beings and the environment, researchers have investigated several Pb-free solders to replace conventional Sn-Pb solders.[1–4] Sn-Ag-Cu solder is one candidate because of its low melting temperature and sufficient mechanical properties.[5,6] Flip-chip technology has been used since the 1960s[7] and exhibits several advantages, such as high input/output connects, low cost, high-frequency performance, and easy assembly. It has become one of the most attractive processing methods used in microelectronics.[8,9]

In the flip-chip technology, multilayered thin-film metallization is used in the under bump metallization (UBM) as the bonding pad on Si chips. Thin-film UBMs are crucial due to their low residual stress, which diminishes the risk of Si cratering around the metallization.[10] The Al/Ni(V)/Cu UBM is currently applicable in flip-chip technology when Sn-Ag-Cu solder is used.[10–13] In this UBM, Cu acts as a wetting layer for the solder while Ni(V) is an efficient barrier layer against solder diffusion.

Recently, the interfacial reactions between Sn-Ag-Cu solder and Al/Ni(V)/Cu UBM after multiple reflows and aging tests were reported.[10–13] However, the literature data concerning the effect of Cu concentration on the interfacial reactions between Sn-Ag-Cu solder and Al/Ni(V)/Cu UBM is limited.[14] In addition, metallurgical studies on assembled Sn-Ag-Cu packages are still lacking.[11,12] The aim of this study is to investigate in detail the interfacial reactions and compound formation in assembled Sn-3.0Ag-(0.5 or 1.5)Cu packages during aging at 150°C. Because the material systems of the UBM on the chip and plastic substrate are different, interfacial reactions near the chip and substrate sides were evaluated, respectively. In addition, the influence

(Received August 30, 2005; accepted May 22, 2006)

of Cu concentration on the compound formation near the chip side was also investigated.

## EXPERIMENTAL PROCEDURES

Figure 1 shows the schematic diagram of the flip-chip Sn-3.0Ag-(0.5 or 1.5)Cu solder joint used in this study. A test chip with ball-shaped Sn-3.0Ag-(0.5 or 1.5)Cu solder bumps was flipped over and assembled to a bismaleimide triazine (BT) substrate with Sn-3.0Ag-0.5Cu pre-solder bumps. The interconnection line on the Si chip was sputtered with 1 μm of Cu; 1.2 μm Al was then sputtered onto the Cu conductor. A trilayer of Al/Ni(V)/Cu thin film was then sputtered onto the metallized substrate to form an UBM structure. The thicknesses of Al, Ni(V), and Cu were 1.2 μm, 1.0 μm, and 0.5 μm, respectively. After the UBM was deposited onto the Si wafer, the Sn-3.0Ag-(0.5 or 1.5)Cu solder paste was stencil-printed on the Al/Ni(V)/Cu UBM and then reflowed at 240°C. The diameter of the flip-chip solder bump was 100 μm. On the BT substrate, Sn-3.0Ag-0.5Cu solder paste was stencil-printed on the electroless Ni-P (EN)/immersion Au finished bonding pads, followed by a reflow step at 240°C. The electroless Ni-P and immersion Au layers were ~5 and 0.1 μm thick, respectively, and the diameter of bonding pad on the BT substrate was 90 μm. After assembly, the gaps between the Si chip and the BT substrate were filled with underfills.

The as-assembled samples were aged at 150°C for 168 h, 500 h, 1,000 h, 1,500 h, and 2,000 h, respectively. The as-assembled and aged samples were first cold-mounted in epoxy and then sectioned by a slow-speed diamond saw. The cross-sectional samples were ground, polished, and etched with 1 part hydrochloric acid/9 parts methanol at room temperature for interfacial analysis. The interfacial morphologies at the chip side and BT substrate side were analyzed by field-emission scanning electron microscopy (FE-SEM, JSM-6500F, JEOL, Japan Electron Optics Laboratory, Tokyo, Japan). Phase compositions in the solder joints and elemental distributions across the joint interfaces were quantitatively measured with a conventional electron probe microanalyzer (EPMA, JXA-8800M, JEOL) with the aid of a ZAF (Z = atomic number factor, A = absorption factor, F = characteristic fluorescence correction) program,[15] as well as a newly developed field-emission EPMA (FE-EPMA 8500F, JEOL). Additional x-ray color mapping images of the solder joints were made with FE-EPMA.

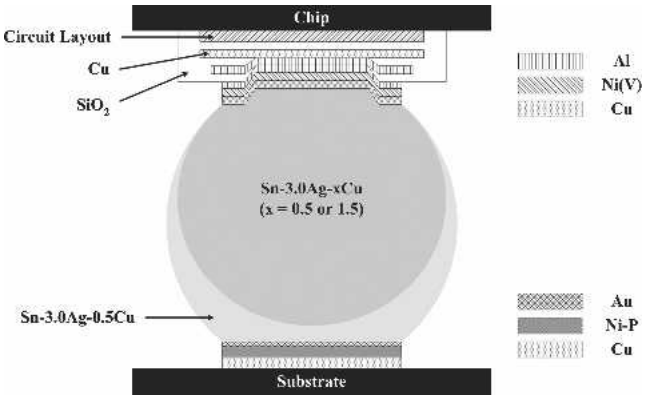


Fig. 1. Schematic illustration of the flip-chip Sn-3.0Ag-(0.5 or 1.5)Cu solder joint employed in this study. The test chip with ball-shaped Sn-3.0Ag-(0.5 or 1.5)Cu solder bumps was flipped over and assembled to a bismaleimide triazine (BT) substrate with Sn-3.0Ag-0.5Cu pre-solder bumps. A sputtered trilayer of a 1.2 μm Al/1.0 μm Ni(V)/0.5 μm Cu thin film was used as the UBM structure on the chip. In addition, the surface finish on the Cu pad at the BT substrate was the electroless Ni-P(5 μm)/immersion Au(0.1 μm) structure.

## RESULTS AND DISCUSSION

### Interfacial Morphology and Phase Identification of As-Assembled Sn-Ag-Cu Joints

The cross-sectional morphology near the chip side in the as-assembled Sn-3.0Ag-0.5Cu joint is exhibited in Fig. 2a. Only one scalloped-type interfacial product was found between the solder and Ni(V) layer after assembly. In consideration of the activation volume caused by the interaction between the electron beam in EPMA and the material under investigation, the size of the interfacial product is near the detection limit of the EPMA, i.e., ~1 μm.[15] To achieve a reliable quantitative result, the appropriate accelerating voltage, beam current, and focused-beam size were deliberately selected in the EPMA analysis.[16] Note that the reported compositions listed in this study are the averages of at least 10 measured points. The average composition (in at.%) of scalloped-type interfacial product was 45.9Sn-36.6Cu-17.5Ni. The ratio of the atomic percentage of (Cu + Ni) to Sn was (36.6 + 17.5)/45.9, which is close to 6:5. Hence, this interfacial product could be denoted as $(Cu_{1-y},Ni_y)_6Sn_5$. The Ni content in the $(Cu_{1-y},Ni_y)_6Sn_5$ IMC varied between 15.8 and 17.5 at.% (i.e., y = 0.29–0.32).

In the case of the as-assembled Sn-3.0Ag-1.5Cu joint, only scalloped-type interfacial product formed near the chip side (Fig. 2b). After EPMA quantitative analysis, the interfacial product was also identified as the $(Cu_{1-y},Ni_y)_6Sn_5$ IMC. However, the concentration of dissolved Ni in $(Cu_{1-y},Ni_y)_6Sn_5$ for the as-assembled Sn-3.0Ag-1.5Cu joint changed from 3.0 to 6.1 at.% (i.e., y = 0.05–0.11), which was less than that in the as-assembled Sn-3.0Ag-0.5Cu joint.

In the as-assembled Sn-3.0Ag-0.5Cu joint, the Cu layer was exhausted and white patches were observed in the Ni(V) layer (Fig. 2a). White patches were also observed between Sn-3.5Ag-1.0Cu and Al/Ni(V)/Cu UBM after 5 reflows in Tu's study.[10] The white patches were denoted as Sn patches. Sn patches are thinner than the EPMA detection limit, i.e., ~1 μm.[15] To obtain reliable quantitative data, the composition of Sn patches was further measured with a newly developed FE-EPMA procedure and was (numbers in at.%) 31.8Al-11.7Ni-37.0Sn-11.1Cu-8.4V. For the as-assembled Sn-3.0Ag-1.5Cu joint, the Cu layer was depleted and converted to $(Cu_{1-y},Ni_y)_6Sn_5$. However, the Ni(V) layer remained intact (Fig. 2b).

With respect to the substrate side in the Sn-3.0Ag-(0.5 or 1.5)Cu joints, the interfacial product between solder and EN was identified as $(Cu_{1-y},Ni_y)_6Sn_5$ with the aid of EPMA (Fig. 3). Ni content in the $(Cu_{1-y},Ni_y)_6Sn_5$ for Sn-3.0Ag-0.5Cu joint was between 18.5 at.% and 23.7 at.% (y = 0.34–0.44). On the other hand, in the $(Cu_{1-y},Ni_y)_6Sn_5$ for the Sn-3.0Ag-1.5Cu joint, dissolved Ni ranged between 17.0 at.% and 23.7 at.% (y = 0.31–0.44).

High-magnification back-scattered electron imaging (BEI) for the Sn-3.0Ag-1.5Cu joint (Fig. 4) clearly showed that two interfacial products formed in the interface of $(Cu_{1-y},Ni_y)_6Sn_5$ and EN, in which the size was smaller than the EPMA detection limit. The compositions of these products were further measured with FE-EPMA. The average composition of the interfacial products (in at.%) was 56.1Sn-10.5Cu-33.4Ni. The ratio of (Ni + Cu) to Sn was close to 3:4; and the interfacial product adjacent to $(Cu_{1-y},Ni_y)_6Sn_5$ could then be considered to be a $(Ni_{1-x},Cu_x)_3Sn_4$ IMC. The Cu content in $(Ni_{1-x},Cu_x)_3Sn_4$ was maintained at ~10.5 at.% (x = 0.24). The composition (in at.%) of interfacial product close to the EN layer was 5.9Sn-72.5Ni-20.6P-1.0Cu. It is evident that P enrichment occurs near the interface of the EN/solder. Because of the Ni diffusion from the EN toward the solder, P is left behind and segregated near the interface of the EN/solder. For the as-assembled Sn-3.0Ag-0.5Cu joint, $(Ni_{1-x},Cu_x)_3Sn_4$ and P-rich layers also formed between the $(Cu_{1-y},Ni_y)_6Sn_5$ and EN layers.

## Interfacial Reaction at the Chip Side during Aging

After assembly, the Sn-3.0Ag-(0.5 or 1.5)Cu joints were aged at 150°C for 168 h, 500 h, 1,000 h,

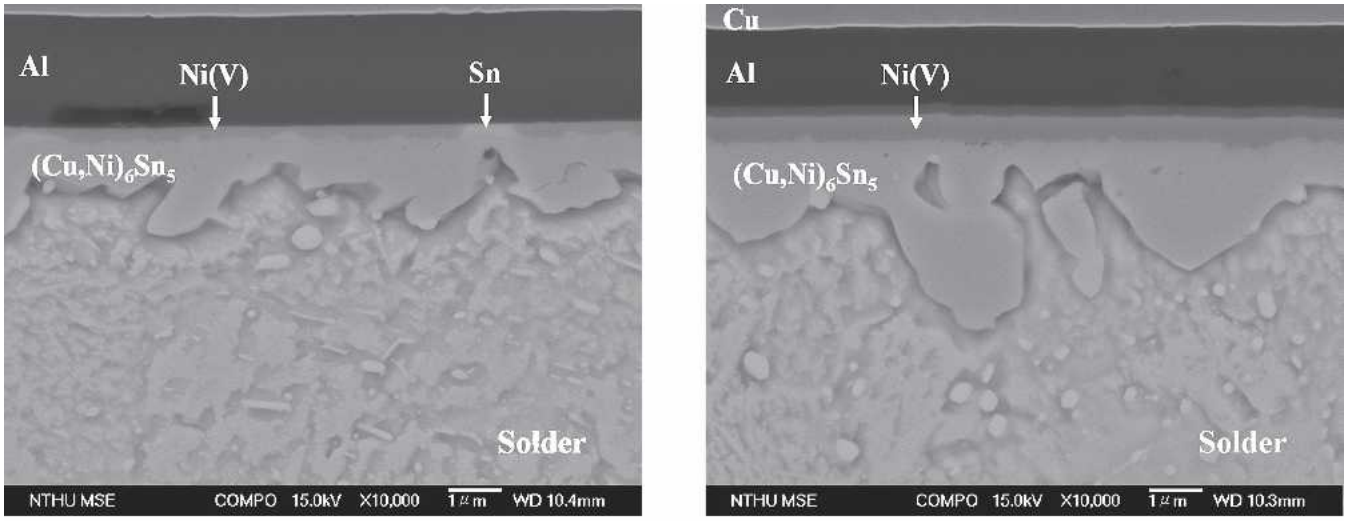


a b

Fig. 2. Cross-sectional image of interfacial morphology at the chip side in the as-assembled flip-chip joints: (a) Sn-3.0Ag-0.5Cu; (b) Sn-3.0Ag-1.5Cu.

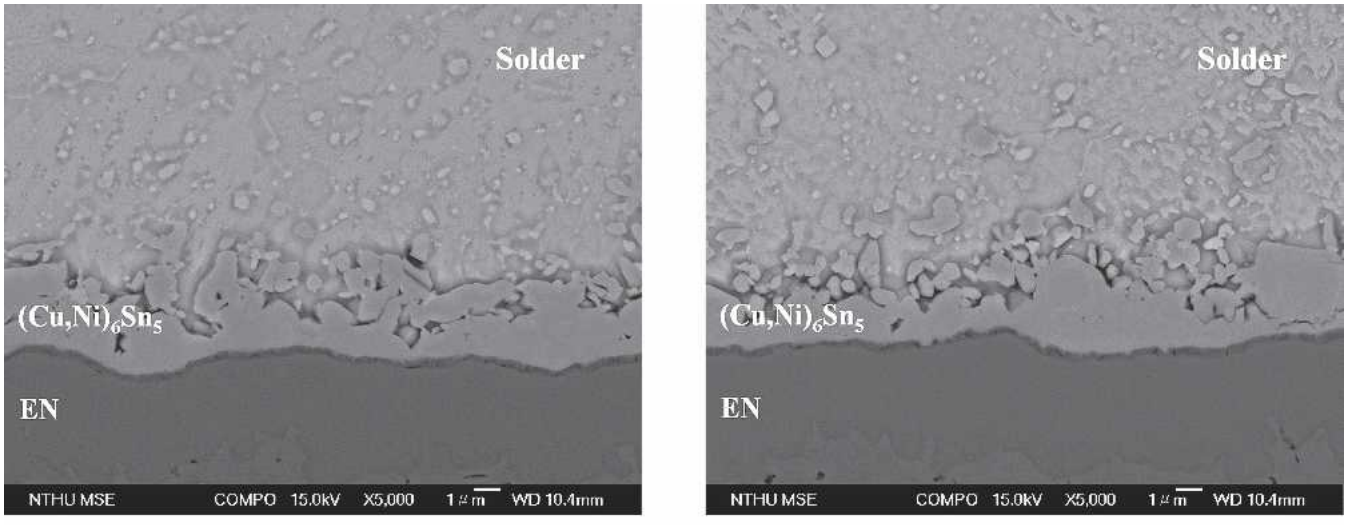


a b

Fig. 3. Cross-sectional image of interfacial morphology at the substrate side in the as-assembled flip chip joints: (a) Sn-3.0Ag-0.5Cu; (b) Sn-3.0Ag-1.5Cu.

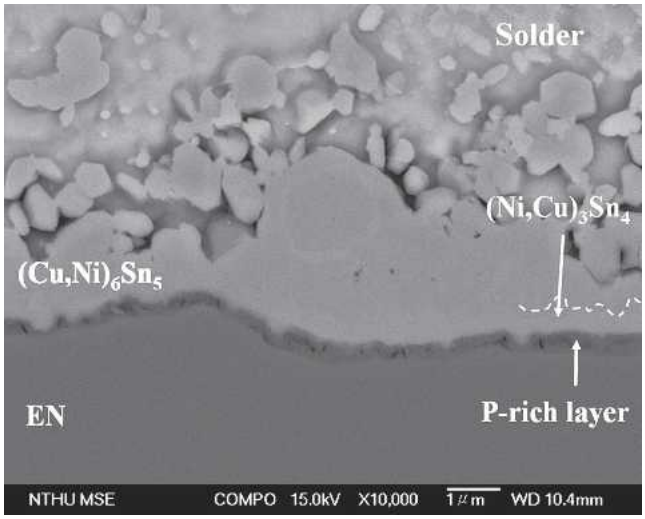


Fig. 4. BEI showing the interfacial morphology at the substrate side in the as-assembled Sn-3.0Ag-1.5Cu joint.

1,500 h, and 2,000 h, respectively. Typical interfacial morphologies at the chip side of Sn-3.0Ag-0.5Cu joints aged for various time are presented in Fig. 5. The scalloped-type interfacial product between solder and UBM was identified as $(Cu_{1-y},Ni_y)_6Sn_5$ with the aid of EPMA. The composition of $(Cu_{1-y},Ni_y)_6Sn_5$ IMC at the chip side was not unique, as shown in Table I. In addition, the Ni(V) layer was gradually consumed during aging (Fig. 5), but the amount of Sn patches increased with aging time. The area fraction (in %) of Sn patches to [Ni(V) layer + Sn patches] after 168 h, 500 h, 1,000 h, 1,500 h, and 2,000 h of aging was 17.4, 18.6, 21.8, 24.1, 32.0, and 61.6, respectively.

Interfacial product formed adjacent to the $(Cu_{1-y},Ni_y)_6Sn_5$ IMC (Fig. 5b–d). After EPMA quantitative analysis, the composition of white product (numbers in at.%) was (25.0 ± 0.8)Sn-(74.2 ± 0.7)Ag-(0.8 ± 0.1)Cu, and the ratio of (Ag + Cu) to Sn approached 3:1. The white product was thus

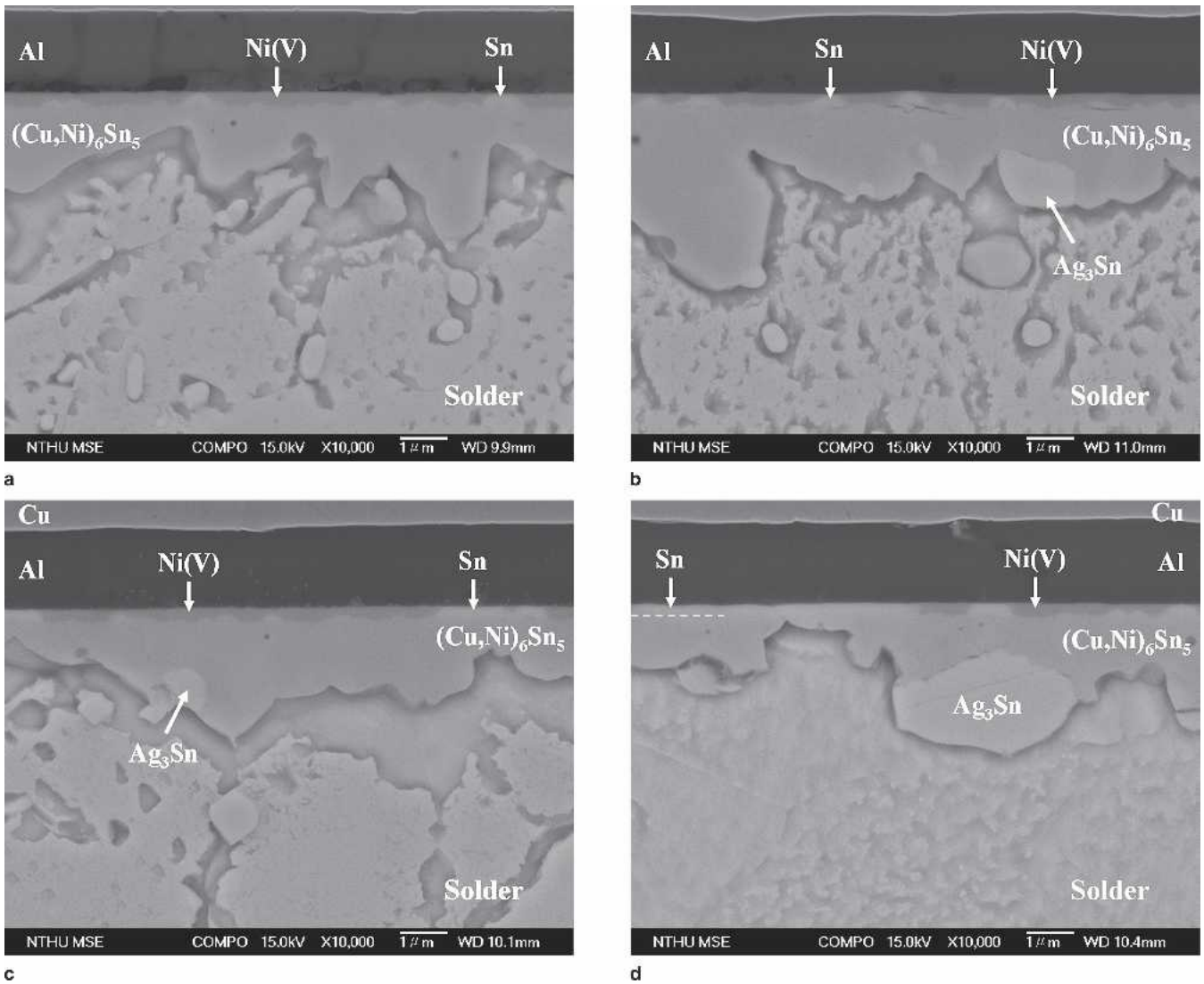


Fig. 5. Cross-sectional image of interfacial morphology at the chip side in the Sn-3.0Ag-0.5Cu joints after aging at 150°C for various times: (a) 168 h, (b) 500 h, (c) 1,000 h, and (d) 2,000 h.

considered to be $Ag_3Sn$ with a small amount of dissolved Cu. The crystal structure of Cu is fcc, identical to that of Ag. The atomic radii of Cu and Ag are 0.128 nm and 0.144 nm, respectively. The atomic radius of Cu is thus 11.1% smaller than that of Ag. The difference in atomic radii between Cu and Ag is less than the limit proposed by Hume-Rothery rule, which indicates that extensive solid solubility of one metal in another occurs only if the radii of the metals differ by <15%.[17] As a result, some Ag in $Ag_3Sn$ IMC could be substituted by Cu.

**Table I. Measured y Values in $(Cu_{1-y},Ni_y)_6Sn_5$ IMCs Formed near Chip and Substrate Sides in Sn-3.0Ag-(0.5 or 1.5)Cu Joints Aged at 150°C**

| | Sn-3.0Ag-0.5Cu | | Sn-3.0Ag-1.5Cu | |
|---|---|---|---|---|
| Aging Time (h) | Chip Side | Substrate Side | Chip Side | Substrate Side |
| 0 | 0.29–0.32 | 0.34–0.44 | 0.05–0.11 | 0.31–0.44 |
| 168 | 0.21–0.32 | 0.34–0.44 | 0.04–0.11 | 0.28–0.44 |
| 500 | 0.21–0.32 | 0.34–0.44 | 0.04–0.11 | 0.20–0.44 |
| 1000 | 0.15–0.32 | 0.27–0.44 | 0.03–0.11 | 0.19–0.44 |
| 1500 | 0.11–0.32 | 0.24–0.44 | 0.03–0.11 | 0.18–0.44 |

For the Sn-3.0Ag-1.5Cu joints, a $(Cu_{1-y},Ni_y)_6Sn_5$ IMC also formed between solder and UBM during 2,000 h of aging (Fig. 6). The value of y in $(Cu_{1-y},Ni_y)_6Sn_5$ at the chip side in the Sn-3.0Ag-1.5Cu joints was altered and smaller than that in the Sn-3.0Ag-0.5Cu joints (Table I). On the other hand, the Ni(V) layer of Al/Ni(V)/Cu UBM was preserved even after 2,000 h of aging. No Sn patch formed between the interface of solder and UBM, even up to 2,000 h of aging. The thickness of $(Cu_{1-y},Ni_y)_6Sn_5$ IMC at the chip side was measured under specific aging conditions (Table II). The thickness of $(Cu_{1-y},Ni_y)_6Sn_5$ for Sn-3.0Ag-1.5Cu joints was slowly increased with aging time. In the Sn-3.0Ag-0.5Cu joints, the $(Cu_{1-y},Ni_y)_6Sn_5$ IMC gradually grew from 1.10 μm at the as-assembled condition to 1.73 μm at 500 h of aging, and then contracted to 1.36 μm at

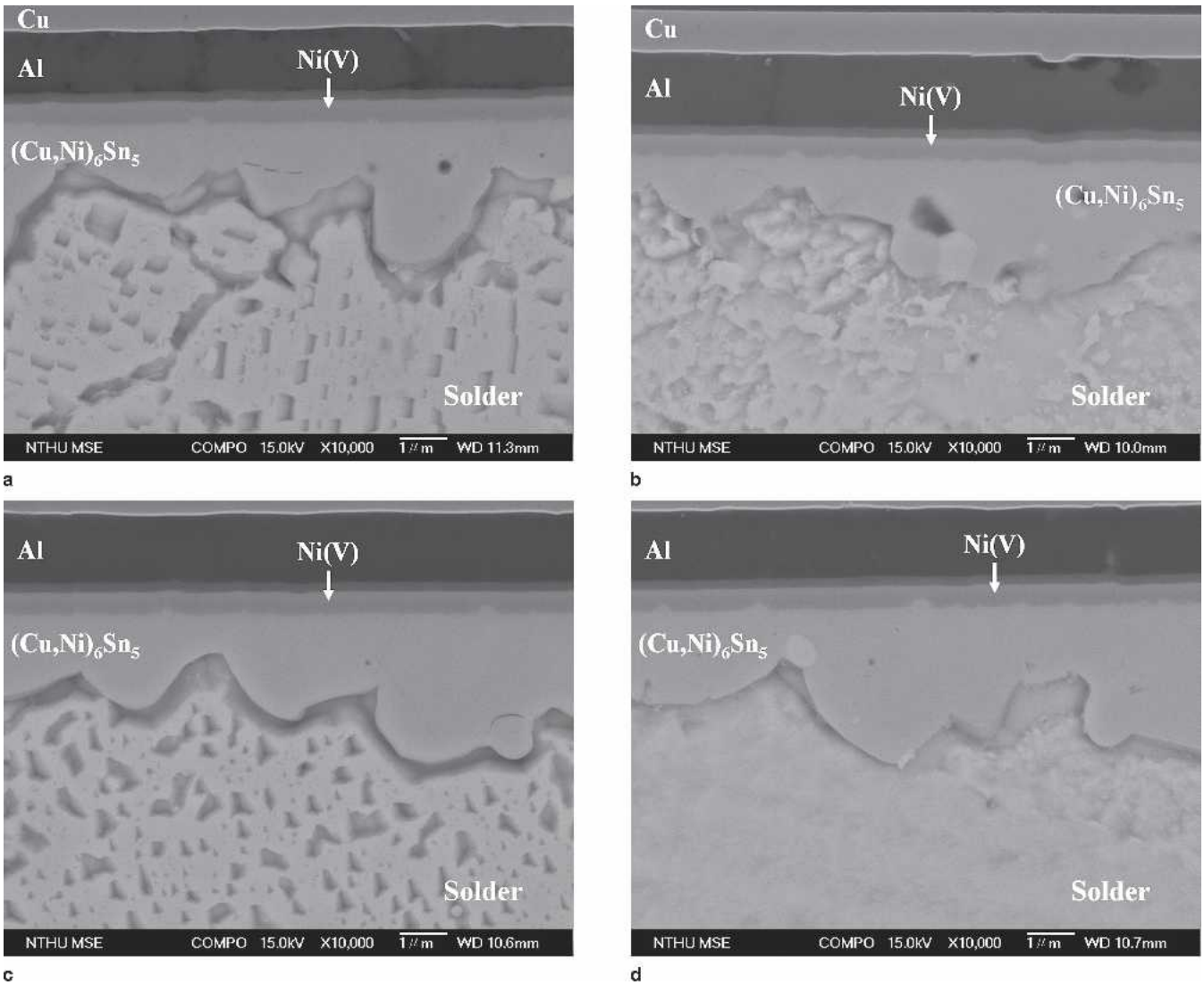


Fig. 6. Cross-sectional image of interfacial morphology at the chip side in the Sn-3.0Ag-1.5Cu joints after aging at 150°C for various times: (a) 168 h, (b) 500 h, (c) 1,000 h, and (d) 2,000 h.

2,000 h of aging. The different growth behavior of the $(Cu_{1-y},Ni_y)_6Sn_5$ IMC between Sn-3.0Ag-0.5Cu and Sn-3.0Ag-1.5Cu systems may be attributed to the formation of Sn patches.

## Interfacial Reaction at the Substrate Side during Aging

During 1,500 h of aging, the interfacial morphologies near the substrate side are similar at various aging times. Figure 7a shows typical interfacial morphology near the substrate side in the Sn-3.0Ag-0.5Cu joints for 500 h of aging. After detailed EPMA composition analysis, the major interfacial product in the interface of solder and EN was identified as $(Cu_{1-y},Ni_y)_6Sn_5$. With the aid of high-magnification BEI, thin, irregular-type and layer-type interfacial products were found between $(Cu_{1-y},Ni_y)_6Sn_5$ and EN after 1,500 h of aging. An enlarged BEI of typical interfacial morphology at the substrate side in the Sn-3.0Ag-0.5Cu joint aged for 500 h is presented in Fig. 8. The thin, irregular-type and layer-type products were confirmed as $(Ni_{1-x},Cu_x)_3Sn_4$ and P-rich layer, respectively, on the basis of quantitative EPMA analysis. After 2,000 h of aging, $(Ni_{1-x},Cu_x)_3Sn_4$ IMC grew to 2.08 $\pm$ 0.41 μm in thickness (Fig. 7b).

For Sn-3.0Ag-1.5Cu joints, the interfacial morphologies at the substrate side are similar at various aging times. The morphologies in the joints after 500 h and 2,000 h are exhibited in Figs. 7c and d, respectively. The major product between solder and

**Table II. Average Thicknes of $(Cu_{1-y},Ni_y)_6Sn_5$ IMC (μm) Formed at the Chip Side for the Sn-3.0Ag-(0.5 or 1.5) Cu Joints Aged at 150°C**

| | Aging Time (h) | | | | | |
|---|---|---|---|---|---|---|
| **Solder Joint** | **0** | **168** | **500** | **1000** | **1500** | **2000** |
| Sn-3.0Ag-0.5Cu | 1.10 | 1.38 | 1.73 | 1.53 | 1.49 | 1.36 |
| Sn-3.0Ag-1.5Cu | 1.52 | 1.86 | 1.86 | 1.96 | 1.97 | 2.06 |

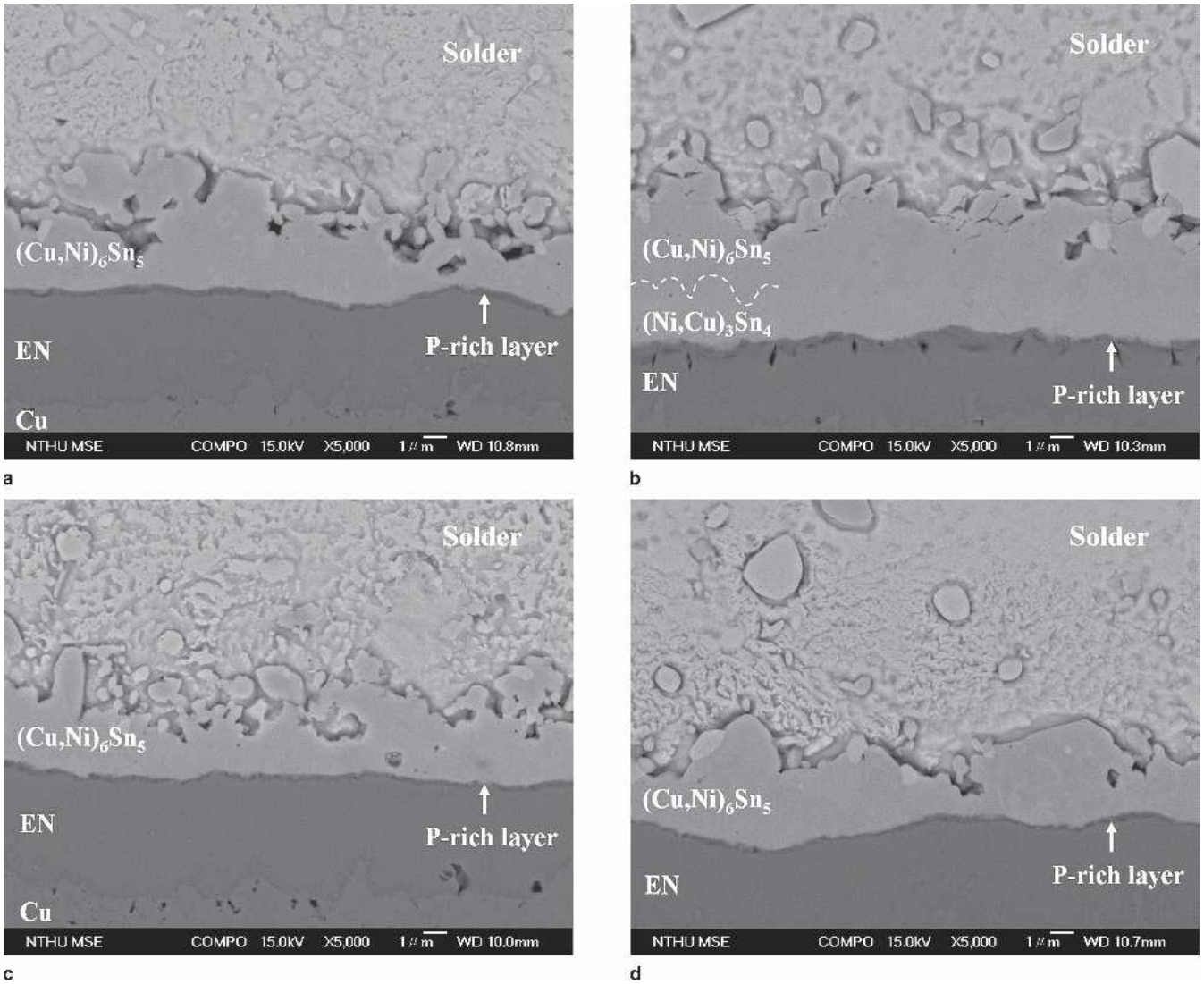


Fig. 7. Cross-sectional image of interfacial morphology at the chip side in the Sn-3.0Ag-0.5Cu joints aged for (a) 500 and (b) 2,000 h and in the Sn-3.0Ag-1.5Cu joints aged for (c) 500 h and (d) 2,000 h.

EN was confirmed as $(Cu_{1-y},Ni_y)_6Sn_5$ IMC. With the aid of high-magnification BEI and FE-EPMA, thin $(Ni_{1-x},Cu_x)_3Sn_4$ IMC and a P-rich layer were also revealed in the interface of $(Cu_{1-y},Ni_y)_6Sn_5$ and EN after 2,000 h of aging.

The thickness of $(Cu_{1-y},Ni_y)_6Sn_5$ IMC at the substrate side was measured in the center of the solder/EN interface (Fig. 9). In the Sn-3.0Ag-1.5Cu joints, $(Cu_{1-y},Ni_y)_6Sn_5$ at the substrate side grew slowly with aging time. The thickness of $(Cu_{1-y},Ni_y)_6Sn_5$ in the Sn-3.0Ag-0.5Cu joints also increased with increasing aging time up to 1,500 h. Nevertheless, the thickness of $(Cu_{1-y},Ni_y)_6Sn_5$ was maintained at ~3.4 μm after >1,500 h. This may be attributed to the growth of $(Ni_{1-x},Cu_x)_3Sn_4$ IMC.

### Effect of Cu Content in Solder on Formation of $(Cu_{1-y},Ni_y)_6Sn_5$ IMC near the Chip Side during Assembly

As mentioned before, the amount of dissolved Ni in $(Cu_{1-y},Ni_y)_6Sn_5$ near the chip side for the Sn-3.0Ag-1.5Cu joint was smaller than that for the Sn-3.0Ag-0.5Cu. On the other hand, the thicknesses of the Ni(V) layer were 0.22 ± 0.11 μm in the Sn-3.0Ag-0.5Cu joint and 0.50 ± 0.05 μm in the Sn-3.0Ag-1.5Cu joint, respectively. Therefore, the amount of consumed Ni(V) layer in the Sn-3.0Ag-0.5Cu joint was greater than that in the Sn-3.0Ag-1.5Cu joint. The different interfacial reactions between Sn-3.0Ag-0.5Cu and Sn-3.0Ag-1.5Cu joints could be related to the concentration of Cu in the solder. If the entire Cu layer dissolved into the Sn-Ag-Cu solder, then the Cu concentration (in %) in the molten solder can be calculated as

$$C_{Cu\ in\ solder} = \frac{W_{Cu\ in\ solder\ bump} + W_{Cu\ in\ pre-solder} + W_{Cu\ layer}}{W_{solder\ bump} + W_{pre-solder} + W_{Cu\ layer}} \times 100 \quad (1)$$

where $W_I$ represents the weight of I, and $W_{Cu\ in\ I}$ is the weight of Cu in I. To obtain $W_I$, the density and volume of flip-chip solder bump, pre-solder, and Cu layer are required. The density of Sn-3.0Ag-0.5Cu and Sn-3.0Ag-1.5Cu solder can be obtained by

$$\rho_{Sn-pAg-qCu} = \frac{100}{\frac{100-p-q}{\rho_{Sn}} + \frac{p}{\rho_{Ag}} + \frac{q}{\rho_{Cu}}} \quad (2)$$

where p and q represent the weight percentage of Ag and Cu in solder and $\rho_I$ indicates the density of I. The densities of Sn, Ag, and Cu are 7.30, 10.49, and 8.94 g/cm$^3$, respectively.[18] Therefore, the calculated densities of Sn-3.0Ag-0.5Cu and Sn-3.0Ag-1.5Cu, respectively, are 7.37 and 7.39 g/cm$^3$.

Before the first reflow for the flip-chip solder bump, the Sn-3.0Ag-(0.5 or 1.5)Cu solder bump used in this study exhibited a cylindrical shape, with a height of 90 μm and a diameter of 100 μm. After stencil printing, the pre-solder bump on the substrate also showed a cylindrical shape, 42 μm in height and 90 μm in diameter. The volume and weight of the flip-chip solder bump, pre-solder bump, and Cu layer were calculated and are summarized in Table III. The masses of Cu in the flip-chip solder bump and pre-solder bump are also listed in Table III. The Cu contents in molten solder were estimated to be 0.98 wt.% for Sn-3.0Ag-0.5Cu joint and 1.71 wt.% for Sn-3.0Ag-1.5Cu joint.

On the basis of thermodynamic data for the Sn-Ag-Cu system,[10,19–23] an enlarged Sn corner of the Sn-Ag-Cu ternary isotherm at 240°C was proposed to illustrate the effect of Cu content in solder on the formation of $(Cu_{1-y},Ni_y)_6Sn_5$ IMC near the chip side (see Fig. 10). The saturation solubility of Cu in the molten solder with 3.0 wt.% Ag at 240°C is ~1.51 wt.%, which is larger than the Cu content in molten solder for the Sn-3.0Ag-0.5Cu joint. Therefore, the molten solder in the Sn-3.0Ag-0.5Cu joint will be able to dissolve the Cu layer completely, and the Ni(V) layer will be exposed and then come into contact with the molten solder. The Ni in

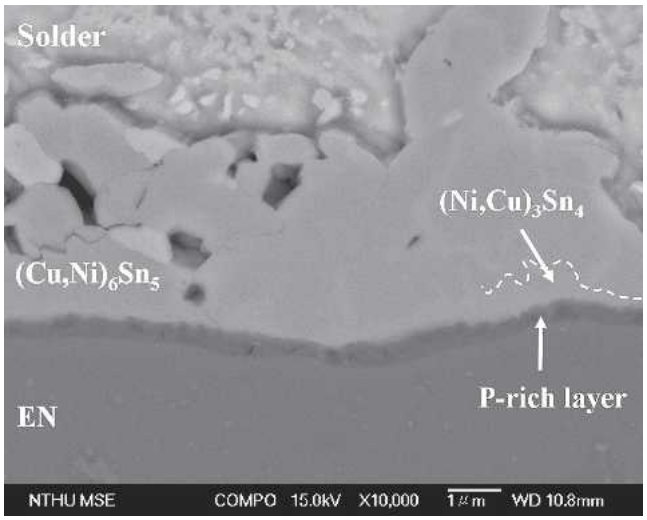


Fig. 8. BEI showing the interfacial morphology at the substrate side in the Sn-3.0Ag-0.5Cu joint aged for 500 h.

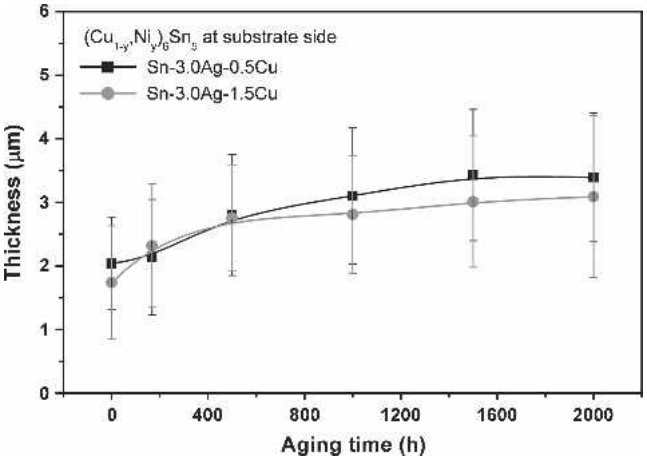


Fig. 9. Thickness of $(Cu_{1-y},Ni_y)_6Sn_5$ IMC formed at the substrate side for Sn-3.0Ag-(0.5 or 1.5)Cu joints aged at 150°C.

**Table III. Calculated Weight of Flip-Chip Solder Bump, Pre-solder Bump, and Cu Layer in the UBM and Calculated Weight of Cu in Flip-Chip Solder Bump, Pre-solder Bump, and Cu Layer**

| I | $\rho_I$ (g/cm$^3$) | $V_I$ (cm$^3$) | $W_I$ (g) | $W_{Cu\ in\ I}$ (g) |
|---|---|---|---|---|
| Sn-3.0Ag-0.5Cu solder bump | 7.37 | $7.07 \times 10^{-7}$ | $5.21 \times 10^{-6}$ | $2.61 \times 10^{-8}$ |
| Sn-3.0Ag-1.5Cu solder bump | 7.39 | $7.07 \times 10^{-7}$ | $5.22 \times 10^{-6}$ | $7.83 \times 10^{-8}$ |
| Sn-3.0Ag-0.5Cu pre-solder | 7.37 | $2.67 \times 10^{-7}$ | $1.97 \times 10^{-6}$ | $9.85 \times 10^{-9}$ |
| Cu layer | 8.94 | $3.93 \times 10^{-9}$ | $3.51 \times 10^{-8}$ | |

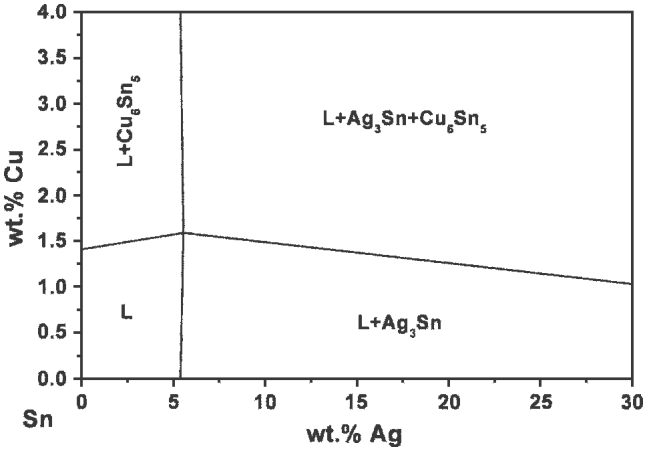


Fig. 10. Enlarged Sn corner of the Sn-Ag-Ni ternary isotherm at 240°C (see Refs. 10 and 19–23).

the Ni(V) layer will thus dissolve into the molten solder and result in the formation of the $(Cu_{1-y},Ni_y)_6Sn_5$ IMC with a higher Ni content. With respect to the Sn-3.0Ag-1.5Cu joint, if the Cu layer completely dissolved into molten solder, then the Cu content in solder was 1.71 wt.%, which was greater than the saturation limit at 240°C. Therefore, only some parts of the Cu layer are dissolved into the molten solder. After the Cu content in molten solder reaches its saturation limit, the remaining Cu layer will react with solder to form $Cu_6Sn_5$ IMC on the Ni(V) layer. Because the Ni(V) layer is not exposed to the liquid phase of the Sn-3.0Ag-1.5Cu solder, the Ni was incorporated into the $Cu_6Sn_5$ IMC through slow solid-state diffusion, resulting in preservation of most of the Ni(V) layer. The dissolved Ni in $(Cu_{1-y},Ni_y)_6Sn_5$ IMC for Sn-3.0Ag-1.5Cu joint was thus less than that for Sn-3.0Ag-0.5Cu joint.

## Diffusion Path Evolution in $(Cu_{1-y},Ni_y)_6Sn_5$ IMC near the Chip Side during Aging at 150°C

Compositions of the $(Cu_{1-y},Ni_y)_6Sn_5$ IMC near the chip side in the Sn-3.0Ag-(0.5 or 1.5)Cu joints after various aging times are summarized in Table I. At the chip side, the maximum values of y in $(Cu_{1-y},Ni_y)_6Sn_5$ were 0.32 for Sn-3.0Ag-0.5Cu joints and 0.11 for Sn-3.0Ag-1.5Cu joints at all aging times. However, the minimum value of y in $(Cu_{1-y},Ni_y)_6Sn_5$ for both Sn-Ag-Cu joints varied with aging time.

To investigate the detailed variation of the composition of Ni in the $(Cu_{1-y},Ni_y)_6Sn_5$ IMC near the chip side, several electron microprobe trace points were set from $(Cu_{1-y},Ni_y)_6Sn_5$ adjacent to the Ni(V) layer into $(Cu_{1-y},Ni_y)_6Sn_5$ near the solder. Typical location and quantitative analysis results for trace points in the Sn-Ag-Cu joints aged for 1,500 h are presented in Fig. 11 and Table IV. In the Sn-3.0Ag-1.5Cu joint aged for 1,500 h, the value of y in $(Cu_{1-y},Ni_y)_6Sn_5$ decreased from 0.11 at the $(Cu_{1-y},Ni_y)_6Sn_5$/UBM interface to 0.03 at the solder/$(Cu_{1-y},Ni_y)_6Sn_5$ interface. For joints aged for 168, 500, and 1,000 h, the value of y in $(Cu_{1-y},Ni_y)_6Sn_5$ was reduced from 0.11 at the $(Cu_{1-y},Ni_y)_6Sn_5$/UBM interface toward specific minimum concentrations at the solder/$(Cu_{1-y},Ni_y)_6Sn_5$ interface (Table I).

For the Sn-3.0Ag-0.5Cu joint aged >1,500 h, the value of y in $(Cu_{1-y},Ni_y)_6Sn_5$ near the UBM was ~0.32 and decreased to 0.11 when approaching the solder side (Fig. 11b and Table IV). However, the value of y in $(Cu_{1-y},Ni_y)_6Sn_5$ close to the UBM was maintained at ~0.32 for various aging times and was then reduced to the minimum value at the solder/$(Cu_{1-y},Ni_y)_6Sn_5$ interface (Table I).

According to phase equilibrium data of the Sn-Cu-Ni system,[24–29] a Sn-$Cu_6Sn_5$-$Ni_3Sn_4$ ternary-phase region in the Sn-Cu-Ni ternary isotherm was proposed to discuss the diffusion path in the $(Cu_{1-y},Ni_y)_6Sn_5$ IMC near the chip side. The maximum and minimum concentrations of Ni dissolved in $(Cu_{1-y},Ni_y)_6Sn_5$ at different aging times were mapped to the ternary isotherm (Fig. 12). In the Sn-3.0Ag-1.5Cu joints, the diffusion path after assembly began at $(Cu_{0.89},Ni_{0.11})_6Sn_5$ (point I1) adjacent to the UBM and continued toward $(Cu_{0.95},Ni_{0.05})_6Sn_5$ close to the solder (point I2), as shown in Fig. 12a. With increasing aging time, the diffusion path in $(Cu_{1-y},Ni_y)_6Sn_5$ IMC changed from path I1–I3 at 168 h of aging to path I1–I4 at 2,000 h of aging.

When the Sn-3.0Ag-0.5Cu joints were aged for fewer than 1,500 h, the diffusion path was also broadened from path J1–J2 after assembly to path J1–J5 at 1,500 h of aging (Fig. 12b). After 2,000 h of aging, the diffusion path in the $(Cu_{1-y},Ni_y)_6Sn_5$ IMC become shorter, i.e., path J1–J6. This may be attributed to the rapid formation of Sn patches after 2,000 h of aging, as discussed before. It should be noted that the ratio of [Sn patches] to [Ni(V) layer + Sn

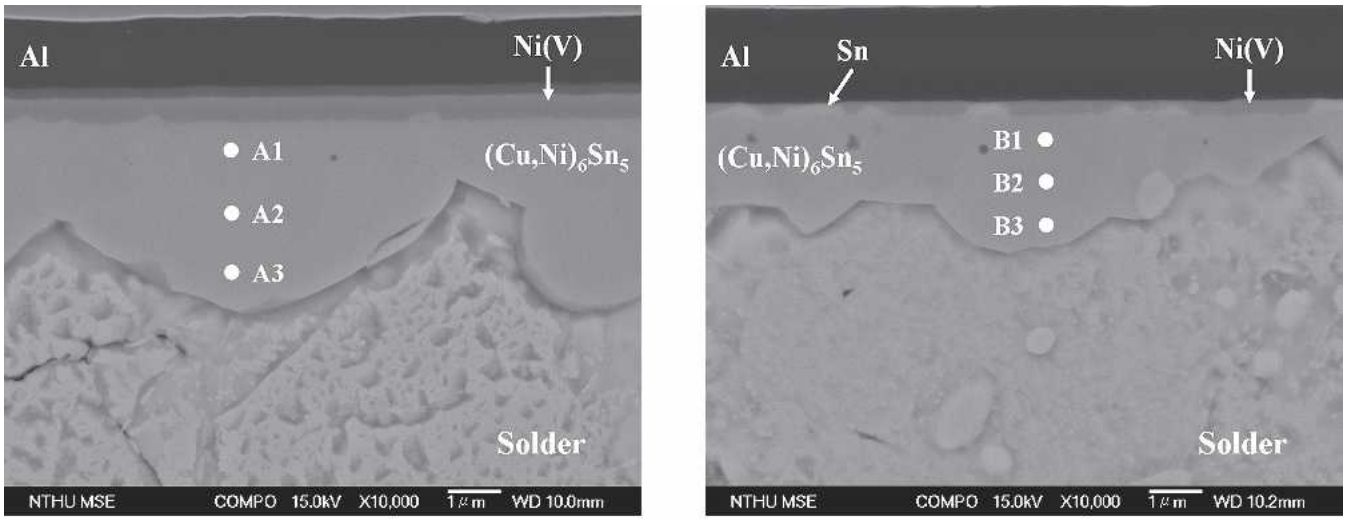


Fig. 11. Cross-sectional image of interfacial morphology at the chip side in solder joints aged for 1,500 h: (a) Sn-3.0Ag-1.5Cu and (b) Sn-3.0Ag-0.5Cu.

**Table IV. Quantitative Analysis Results for Trace Points in Fig. 11 at Chip Side in the Sn-3.0Ag-(0.5 or 1.5)Cu Joints after 1500 h of Aging**

| Measurement Locations | Composition (at.%) | | | IMC |
|---|---|---|---|---|
| | Sn | Cu | Ni | |
| A1 | 45.9 | 48.3 | 5.8 | $(Cu_{0.89},Ni_{0.11})_6Sn_5$ |
| A2 | 46.3 | 49.8 | 3.9 | $(Cu_{0.93},Ni_{0.07})_6Sn_5$ |
| A3 | 46.8 | 51.5 | 1.7 | $(Cu_{0.97},Ni_{0.03})_6Sn_5$ |
| B1 | 46.1 | 36.4 | 17.5 | $(Cu_{0.68},Ni_{0.32})_6Sn_5$ |
| B2 | 45.9 | 41.5 | 12.6 | $(Cu_{0.77},Ni_{0.23})_6Sn_5$ |
| B3 | 46.7 | 47.6 | 5.7 | $(Cu_{0.89},Ni_{0.11})_6Sn_5$ |

patches] increased from 32.0% at 1,500 h of aging to 61.6% at 2,000 h of aging.

## CONCLUSIONS

- During the assembly process, the Cu layer in the thin-film UBM was exhausted in the Sn-3.0Ag-0.5Cu joint. The Ni(V) layer was thus in contact with molten solder, resulting in formation of $(Cu_{1-y},Ni_y)_6Sn_5$ IMC.
- Some portion of the Ni(V) layer was replaced with Sn patches in the Sn-3.0Ag-0.5Cu joints. With increasing aging time, the Ni(V) layer was gradually consumed, and the ratio of [Sn patches] to [Ni(V) layer + Sn patches] increased to 61.6% at 2,000 h of aging.
- For the Sn-3.0Ag-1.5Cu joint, only some portions of Cu layer were dissolved into molten solder during assembly. Therefore, the remaining Cu layer rapidly reacted with solders to form $Cu_6Sn_5$, which completely covered the Ni(V) layer. Ni from the Ni(V) layer was incorporated into the $Cu_6Sn_5$ IMC through slow solid-state diffusion. Thus the concentration of Ni in $(Cu_{1-y},Ni_y)_6Sn_5$ was thus less than that in the Sn-3.0Ag-0.5Cu joint.

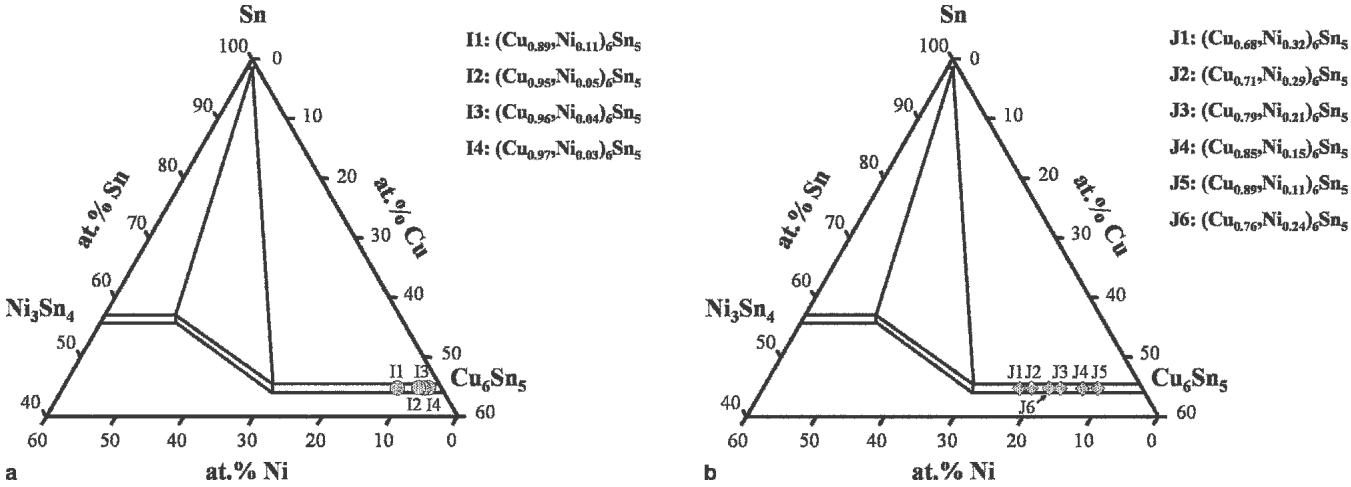


Fig. 12. Sn-$Cu_6Sn_5$-$Ni_3Sn_4$ ternary-phase region in the Sn-Cu-Ni isotherm. Compositions of $(Cu_{1-y},Ni_y)_6Sn_5$ near the chip side for various aging times are mapped to isotherms in (a) Sn-3.0Ag-1.5Cu joints and (b) Sn-3.0Ag-0.5Cu joints.

- With respect to the interfacial reaction near the substrate side, $(Cu_{1-y},Ni_y)_6Sn_5$, $(Ni_{1-x},Cu_x)_3Sn_4$, and P-rich layer formed between solder and EN for both Sn-Ag-Cu joints after assembly and aging. The major interfacial product was the $(Cu_{1-y},Ni_y)_6Sn_5$ IMC except for the Sn-3.0Ag-0.5Cu joint aged for 2,000 h. After 2,000 h of aging, $(Ni_{1-x},Cu_x)_3Sn_4$ IMC grew to 2.08 μm, which is a value close to that of the $(Cu_{1-y},Ni_y)_6Sn_5$ IMC in the Sn-3.0Ag-0.5Cu joint.
- The diffusion path in the $(Cu_{1-y},Ni_y)_6Sn_5$ IMC near the chip side was broadened with aging time except for the Sn-3.0Ag-0.5Cu joint aged for 2,000 h. After 2,000 h of aging, the diffusion path in $(Cu_{1-y},Ni_y)_6Sn_5$ became shortened in the Sn-3.0Ag-0.5Cu joint. This can be attributed to the rapid formation of Sn patches after 2,000 h of aging.

## ACKNOWLEDGEMENTS

Financial support and joint assembly by Taiwan Semiconductor Manufacturing Company (TSMC) are acknowledged. Partial support from the National Science Council (under contract no. NSC-93-2216-E007-014) is also appreciated.

## REFERENCES

1. K.S. Bae and S.J. Kim, *J. Mater. Res.* 17, 743 (2002).
2. H.W. Miao and J.G. Duh, *Mater. Chem. Phys.* 71, 255 (2001).
3. D.R. Frear, J.W. Jang, J.K. Lin, and C. Zang, *JOM* 53, 28 (2001).
4. B.L. Young, J.G. Duh, and B.S. Chiou, *J. Electron. Mater.* 30, 543 (2001).
5. K. Suganuma, *Curr. Opin. Solid State Mater. Sci.* 5, 55 (2001).
6. K.S. Kim, S.H. Huh, and K. Suganuma, *Mater. Sci. Eng., A* 333, 106 (2002).
7. L.F. Miller, *IBM J. Res. Dev.* 13, 239 (1969).
8. J.H. Lau, *Flip Chip Technologies* (New York: McGraw-Hill, 1996), pp. 26–30.
9. G.R. Blackwell, *The Electronic Packaging Handbook* (Boca Raton, Florida: CRC Press, 2000), pp. 4.4–4.25.
10. M. Li, F. Zhang, W.T. Chen, K. Zeng, K.N. Tu, H. Balkan, and P. Elenius, *J. Mater. Res.* 17, 1612 (2002).
11. F. Zhang, M. Li, C.C. Chum, and K.N. Tu, *J. Mater. Res.* 17, 2757 (2002).
12. F. Zhang, M. Li, C.C. Chum, and Z.C. Shao, *J. Electron. Mater.* 32, 123 (2003).
13. F. Zhang, M. Li, B. Balakrisnan, and W.T. Chen, *J. Electron. Mater.* 31, 1256 (2002).
14. J.S. Ha, T.S. Oh, and K.N. Tu, *J. Mater. Res.* 18, 2109 (2003).
15. J.I. Goldstein, D.E. Newbury, D.C. Joy, C.E. Lyman, P. Echlin, E. Lifshin, L. Sawyer, and J.R. Michael, *Scanning Electron Microscopy and X-ray Microanalysis* (New York: Plenum, 2003), pp. 391–420.
16. G.Y. Jang, C.S. Huang, L.Y. Hsiao, J.G. Duh, and H. Takahashi, *J. Electron. Mater.* 33, 1118 (2004).
17. R.E. Reed-Hill and R. Abbaschian, *Physical Metallurgy Principles* (Boston: PWS Publishing Company, 1994), pp. 272–299.
18. W.D. Callister, *Materials Science and Engineering: An Introduction* (New York: John Wiley & Sons, Inc., 1997), pp. 8–27.
19. H. Ohtani, K. Okuda, and K. Ishida, *J. Phase Equilib.* 16, 416 (1995).
20. J.H. Shim, C.S. Oh, B.J. Lee, and D.N. Lee, *Z. Metallkd.* 87, 205 (1996).
21. F.H. Hayes, H.L. Lukas, G. Effenberg, and G. Petzow, *Z. Metallkd.* 77, 749 (1986).
22. C.S. Oh, J.H. Shim, B.J. Lee, and D.N. Lee, *J. Alloys Compd.* 238, 155 (1996).
23. K.W. Moon, W.J. Boettinger, U.R. Kattner, F.S. Biancaniello, and C.A. Handwerker, *J. Electron. Mater.* 29, 1122 (2000).
24. C.H. Lin, S.W. Chen, and C.H. Wang, *J. Electron. Mater.* 31, 907 (2002).
25. W.T. Chen, C.E. Ho, and C.R. Kao, *J. Mater. Res.* 17, 263 (2002).
26. C.Y. Li and J.G. Duh, *J. Mater. Res.* 20, 3118 (2005).
27. T.B. Massalski, H. Okamoto, P.R. Subramanian, and L. Kacprzak, *Binary Alloy Phase Diagrams* (Materials Park, Ohio: ASM Int., 1990), pp. 1442–1446.
28. T.B. Massalski, H. Okamoto, P.R. Subramanian, and L. Kacprzak, *Binary Alloy Phase Diagrams* (Materials Park, Ohio: ASM Int., 1990), pp. 2863–2864.
29. T.B. Massalski, H. Okamoto, P.R. Subramanian, and L. Kacprzak, *Binary Alloy Phase Diagrams* (Materials Park, Ohio: ASM Int., 1990), pp. 1481–1483.